

# EXPERIMENTAL INVESTIGATION OF FLOW FEATURES AND ACOUSTIC RADIATION OF A ROUND CAVITY UNDER SUBSONIC GRAZING FLOW.

*O. Marsden, E. Jondeau, P. Souchotte, and C. Bailly*

*Laboratoire de Mécanique des Fluides et d'Acoustique  
Ecole Centrale de Lyon & UMR CNRS 5509  
36 avenue Guy de Collongue, 69134 Ecully cedex, France*

March 14, 2008

## 1 Introduction

Over the past few decades, aircraft jet noise has seen a progressive but significant reduction, as a side effect of the sustained increase in bypass ratio. This has led to renewed interest in the remaining aeroacoustic noise sources around an aircraft, as they are now the principal contributors to perceived noise during landing phases.

Flow-excited cavities are known to be one of the main generic noise generators on an airframe. A number of studies in the past have examined the flow and acoustic field around rectangular cavities. The interested reader is referred to two comprehensive reviews in particular [1, 2]. However, cylindrical cavities have been the focus of far less attention. In this work, we present experimental results regarding a cylindrical cavity grazed by a turbulent boundary layer. This geometry is often encountered on the pressure side of commercial aeroplane wings. Fuel overpressure outlets are a common example, and contribute to airframe noise during approach phases. The current work investigates the boundary layer flow over round cavities and the radiated noise for various aspect ratios and free-stream velocities.

The present work is organized as follows. A brief description of the experimental set-up is given in Section . Some results and discussions can be found in Section , followed by concluding remarks and outlook.

## 2 Experimental Setup

Cavity noise experiments were conducted in the high-speed anechoic wind tunnel ( $10 \times 8 \times 8 \text{ m}^3$ ) of the Centre Acoustique at the Ecole Centrale de Lyon [3]. A schematic view of the installation can be seen in Figure 1. The flow exits from a rectangular nozzle with a section of 0.5 by 0.25 m, over a flat plate measuring 0.8 m in the streamwise direction by 0.6 m in the

cross-flow direction. The round 10 cm diameter cavity is placed 45 cm downstream from the nozzle exit. In order to obtain a reproducible incoming turbulent boundary layer, a strip of sandpaper is placed inside the nozzle before the convergent zone, thus ensuring a complete transition to a turbulent state for all flow velocities of interest.

The main flow and geometric parameters of the study are listed in table 1. Incoming flow velocity ranges from 50 to 110 m/s, or approximately  $M = 0.15$  to  $M = 0.34$ . The boundary layer thickness  $\delta_{99}$ , also reported in table 1, varies between around 18 mm and 16 mm over this Mach number range, while the shape factor  $H = \delta_*/\delta_\theta \simeq 1.35$ . Turbulence levels in the free-stream are very low, and do not exceed 1% of the free-stream velocity. Maximum levels in the boundary layer are reached at a distance of approximately 3 mm from the wall. Figure 2 shows an example of velocity profiles, both mean and rms fluctuations, measured just upstream of the cavity leading edge by LDA, for the 70 m/s case.

The cavity has been instrumented in order to allow the measurement of both static and fluctuating wall pressure signals. For static wall pressure measurements, 0.7 mm stainless steel tubes are flush-mounted on the cavity walls, and connected to a FURNESS© manometer with atmospheric pressure as reference. These pressure tapings are located along four vertical lines on the cylindrical wall, and along two perpendicular diameters on the cavity floor. The cavity block can be rotated with respect to the grazing flow, allowing to measure static pressure at any angular position around the cavity.

In a similar way, the cavity is fitted with a total of 20 B&K 1/4" microphones, arranged in four vertical lines comprising four microphones each, and 4 microphones on the cavity floor. Again, the instrumented cavity can be rotated with respect to the flow in order to obtain fluctuating pressure measurements anywhere on the cavity walls. Far-field acoustic directivity mea-

surements have also been performed, thanks to seven B&K ICP type 4935 microphones placed on a semi-circular rotating antenna centred on the cavity.

Cavity radius $r$	50 mm
Cavity depths $h$	50, 100, 150 mm
Flow velocities $U_\infty$	50, 70, 90 m/s
Boundary layer thickness $\delta_{99}$	17 mm

Table 1: Main parameters of the flow configuration studied.

### 3 Experimental results & analysis

It is known that deep cylindrical cavities are highly resonant at their quarter-wavelength frequency. The resonant frequency of interest is given by  $f_c = c_0/4(h + \delta_h)$  where  $\delta_h = 0.8216 \times r$  corresponds to the acoustic correction length for an infinitely flanged open pipe [4]. For our reference cavity depth of 100 mm, this leads to a frequency of  $f_c \simeq 607$  Hz. It should be noted however that the aspect ratio  $2r/d$  is equal in this case to one, and in that respect the cavity should not be qualified as deep.

In the context of this study, it is interesting to note that the acoustic PSD has maxima that vary strongly with flow velocity, as shown in Figure 3. In fact, the three spectra in this Figure exhibit markedly different behaviours. Those measured at 50 and 90 m/s show two separate peaks, while that measured at 70 m/s has a single maximum at a frequency of 650 Hz, about 7% higher than  $f_c$ . The single peak observed at 70 m/s is noticeably sharper than the double peaks of the two other spectra. It is thus apparent that at least at 50 and 90 m/s, a depth-mode acoustic resonance of the cavity is not the main noise source.

This observation is seconded by Figure 4 which shows the acoustic power at 1 m as a function of the free-stream flow velocity. It is compared to a  $U_\infty^6$  scaling, shown as the dashed line. Acoustic scaling based on  $U_\infty^6$  is typical of compact dipolar noise source mechanisms, such as turbulent fluctuations close to a rigid surface. Thus a sixth power scaling would be anticipated in the absence of notable acoustic resonance in the cavity, as a result of the shear layer interaction with the downstream wall. The baseline evolution of the acoustic power is well described by this scaling, but it deviates notably from the sixth power law for velocities around 70 m/s and 110 m/s. The additional acoustic power is assumed to be the result of resonant phenomena around these flow velocities.

Figure 5 shows the acoustic PSD at 70 m/s for three different cavity depths, as well as for the baseline flat plate case. For the cavity of 50 mm depth, there is a wide hump in the PSD at around 900-1000 Hz. This frequency range matches the resonant frequency of  $f_c = 942$  Hz for this depth, but the wide-band aspect of the hump suggests that no strong feedback mech-

anism between the shear layer and the acoustic emission is present. For the two deeper cavities, the peaks in the PSD also correspond to the respective resonant frequencies, but the peaks are much narrower, indicating a more resonant phenomenon in these cases.

Figure 6 represents the acoustic PSD, measured at a height of 1 m above the cavity, as a function of the upstream flow velocity  $U_\infty$  and frequency for the 100 mm-deep cavity. Also represented as a solid black line is the quarter-wavelength theoretical resonance frequency of the cavity. Frequencies of the peaks in the PSD vary with velocity, indicating that shear layer modes rather than acoustic pipe resonance are the dominating phenomenon at play. Instead, acoustic resonance appears to modulate the level of noise generated by shear layer modes, as shown by the evolution of the maximum levels. Figure 6 also explains the presence of two peaks at 50 and 90 m/s, there being two active shear layer modes of comparable level at these flow velocities.

A different representation of this information is shown in Figure 7, where the SPL is now represented as a function of upstream velocity and diameter-based Strouhal number  $St = fD/U_\infty$ . Rossiter[5] was the first to propose a physical explanation for tonal noise generation, as well as a semi-empirical relationship predicting discrete Strouhal numbers at which such tones can be observed. Rossiter reasoned that tonal amplification was due to a feedback mechanism between vorticity creation at the cavity leading edge, and the noise emitted by the same vorticity impinging the downstream cavity wall. His relationship

$$St = \frac{fL}{U_\infty} = \frac{n - \alpha}{M + U_\infty/U_c}$$

where  $U_c$  is the average convection velocity of vortical structures in the shear layer and  $\alpha$  is an empirical constant generally taken around 0.25, suggests that tonal amplification can take place for frequencies such that the convection time  $L/U_c$  for vortices across the cavity opening, added to the acoustic propagation time between the downstream and upstream cavity corners,  $L/c_\infty$ , is a multiple of the period, where the multiple  $n$  corresponds to the average number of vortices in the shear layer. This relationship has been shown to work well for a wide variety of different cavity configurations. Its suitability for round cavities is considerably less evident, since the distance  $L$  used in the above expression is no longer constant in the cross-stream direction. It has however been plotted in dotted black lines in Figure 7 for reference, for  $n = 1, 2, \text{ and } 3$ . It can be observed that these Rossiter curves do not accurately represent the variation of the Strouhal number with Mach number. The stars show the Strouhal number corresponding to the round cavity's quarter-wavelength resonant frequency. The maximum acoustic levels for each shear layer mode are found close to the intersection between the quarter-

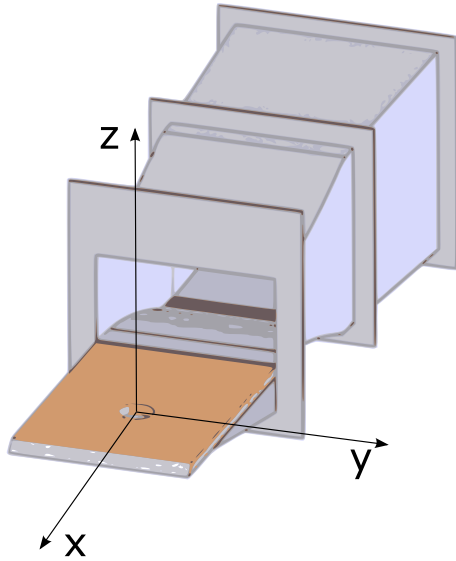
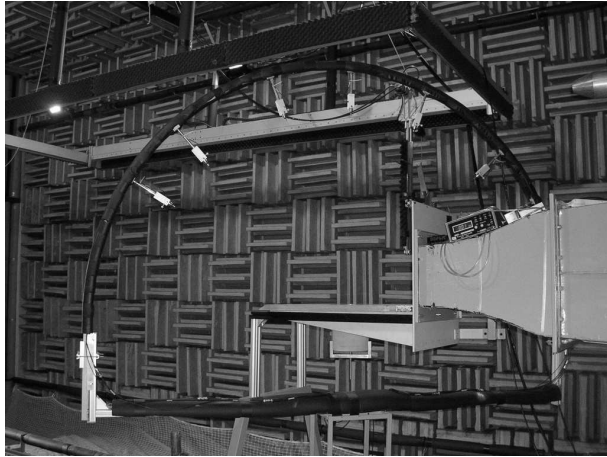


Figure 1: View of the experimental setup

wavelength Strouhal and the shear layer Strouhal. Finally, the blue dashed lines represent the lower and upper Strouhal number bounds for which the imaginary part of the Rayleigh conductivity  $\sigma$  of the cavity mouth is negative. These values are given in the work by Grace *et al.*[6] For a pressure difference fluctuation at a given Strouhal number across an aperture shear layer, a negative value of the imaginary part of the conductivity will lead to the amplification of the periodic pressure difference, while a positive imaginary part will attenuate the pressure difference. Hence it is interesting to note that high acoustic levels are located mostly within these bounds, and in particular that the second shear layer mode reaches its acoustic maximum for  $St = 1.9$  (blue circles), corresponding to the most negative imaginary part of the Rayleigh conductivity.

#### 4 Concluding remarks

Laser Doppler Velocimetry (LDV) measurements have been done to complete the present experimental results and will be presented in future work. The aim

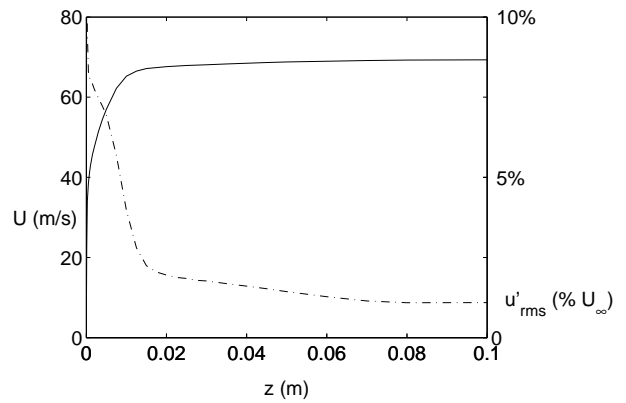


Figure 2: Case  $U_\infty = 70$  m/s. Solid black line: boundary layer profile upstream of the cavity, as a function of  $z$ . Dashed black line: profile of rms fluctuations in the boundary layer, as a function of  $z$ .

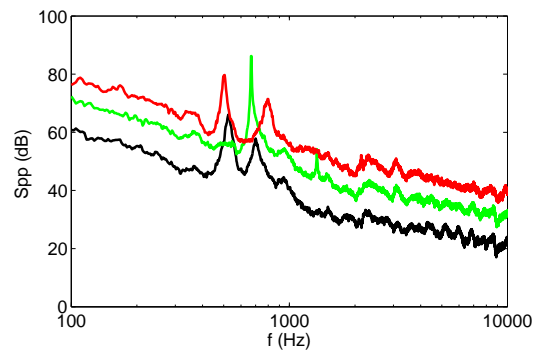


Figure 3: PSD ( $\text{Pa}^2/\text{Hz}$ ) at 1 m above the cavity at three different flow velocities: —  $U_\infty = 50$  m/s, —  $U_\infty = 70$  m/s, —  $U_\infty = 90$  m/s

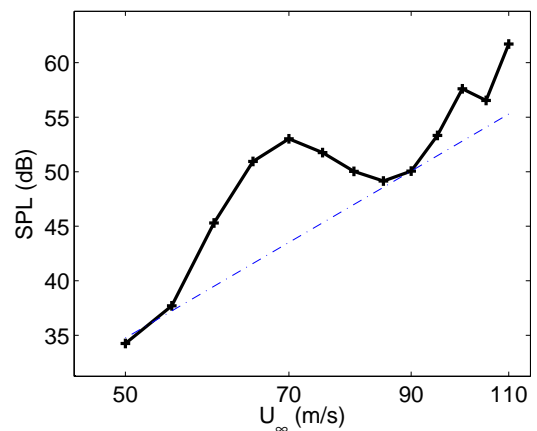


Figure 4: SPL in dB at 1 m above the cavity, as a function of freestream velocity. -+- experimental data, - - -  $U_\infty^6$  scaling

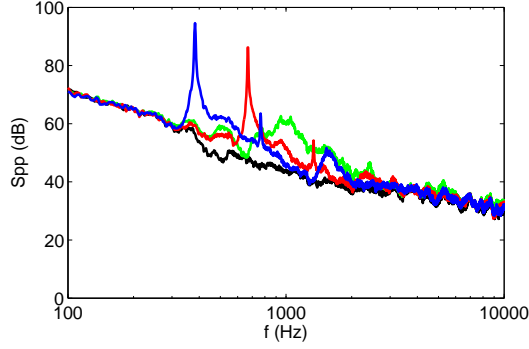


Figure 5: PSD ( $\text{Pa}^2/\text{Hz}$ ) at 1 m, with  $U_\infty = 70 \text{ m/s}$ , for three cavity depths  $h$ : —  $h = 0 \text{ mm}$ , —  $h = 50 \text{ mm}$ , —  $h = 100 \text{ mm}$ , —  $h = 150 \text{ mm}$ .

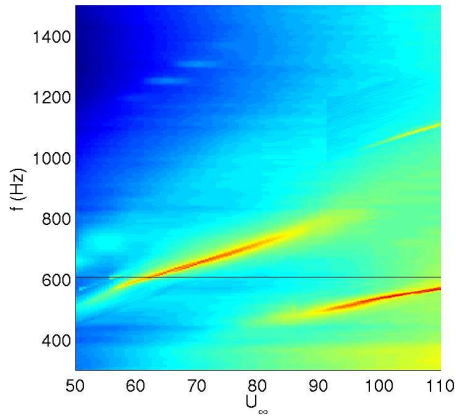


Figure 6: PSD ( $\text{Pa}^2/\text{Hz}$ ) at 1 m represented as a function of velocity. Colour scale between 0 and 60 dB.

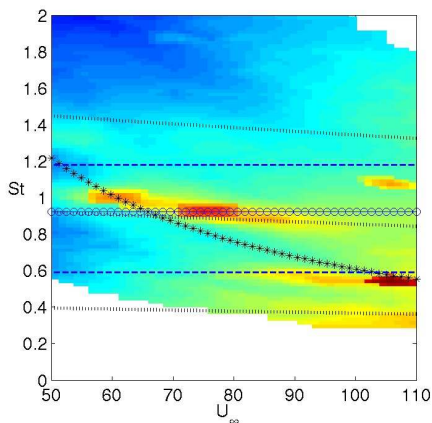


Figure 7: PSD ( $\text{Pa}^2/\text{Hz}$ ) at 1 m represented as a function of velocity and diameter-based Strouhal number. Colour scale between -10 and 50 dB. Dotted black lines show the first three Rossiter modes based on the diameter. Dashed blue lines show the bounds inside which  $\Im(\sigma) < 0$ , and blue circles show its most negative value.

of the present work is to provide a large database of the flow and its acoustics for comparison and validation with future numerical simulations.

## 5 Acknowledgment

This research project is supported by the *Fondation de Recherche pour l'Aéronautique & l'Espace (FRAE)* under contract reference AFB AEROCV, and in collaboration with following french laboratories: ONERA, SINUMEF, IUSTI and INRIA.

## 6 \*

### References

- [1] D. Rockwell and E. Naudascher. Self-sustained oscillations of impinging free shear layer. *Annual Review of Fluid Mechanics*, 11:67–94, 1979.
- [2] T. Colonius. An overview of simulation, modeling and active control of flow/acoustic resonance in open cavities. *AIAA Paper 2001-0076*, 2001.
- [3] M. Sunyach, B. Brunel, and G. Comte-Bellot. Performances de la soufflerie anechoique grande vitesse de l'Ecole Centrale de Lyon. *Revue d'Acoustique*, 73:316–330, 1985.
- [4] Y. Nomura, I. Yamamura, and S. Inawashiro. On the acoustic radiation from a flanged circular pipe. *J. Phys. Soc. Jap.*, 15(3), 1960.
- [5] J.E. Rossiter. Wind-tunnel experiments on the flow over rectangular cavities at subsonic and transonic speeds. Technical Report 3438, *Aeronautical Research Council Reports and Memoranda*, 1964.
- [6] S.M. Grace, K.P. Horan, and M.S. Howe. The influence of shape on the rayleigh conductivity of a wall aperture in the presence of grazing flow. *J. Fluids Struct.*, 12:335–351, 1998.